CONTRIBUTI DI RICERCA CRENOS

SMOOTH AND ABRUPT DYNAMICS IN FINANCIAL VOLATILITY: THE MS-MEM-MIDAS

Luca Scaffidi Domianello
Giampiero M. Gallo
Edoardo Otranto

WORKING PAPERS

2022/05

arkadia

Centro Ricerche Economiche Nord Sud
(CRENoS)
Università di Cagliari
Università di Sassari

CRENOS was set up in 1993 with the purpose of organising the joint research effort of economists from the two Sardinian universities (Cagliari and Sassari) investigating dualism at the international and regional level. CRENoS' primary aim is to improve knowledge on the economic gap between areas and to provide useful information for policy intervention. Particular attention is paid to the role of institutions, technological progress and diffusion of innovation in the process of convergence or divergence between economic areas. To carry out its research, CRENoS collaborates with research centres and universities at both national and international level. The centre is also active in the field of scientific dissemination, organizing conferences and workshops along with other activities such as seminars and summer schools.
CRENoS creates and manages several databases of various socio-economic variables on Italy and Sardinia. At the local level, CRENoS promotes and participates to projects impacting on the most relevant issues in the Sardinian economy, such as tourism, environment, transports and macroeconomic forecasts.

www.crenos.unica.it
crenos@unica.it

CRENoS – Cagliari
Via San Giorgio 12, I-09124 Cagliari, Italia
tel. +39-070-6756397; fax +39-070- 6756402

CRENoS - Sassari
Via Muroni 25, I-07100 Sassari, Italia
tel. +39-079-213511

Title: SMOOTH AND ABRUPT DYNAMICS IN FINANCIAL VOLATILITY: THE MS-MEM-MIDAS

Prima Edizione: Dicembre 2022

ISBN: 978 88 68514 372

Viale Bonaria 98 - 09125 Cagliari
Tel. 070/6848663 - info@arkadiaeditore.it
www.arkadiaeditore.it

Smooth and Abrupt Dynamics in Financial Volatility: the MS-MEM-MIDAS

Luca Scaffidi Domianello[*]
University of Florence
Giampiero M. Gallo[±]
New York University in Florence & CRENoS
Edoardo Otranto[∝]
University of Messina & CRENoS

Abstract

In this paper we remark that the evolution of the realized volatility is characterized by a combination between high–frequency dynamics and a smoother persistent dynamics evolving at a lower–frequency. We suggest a new Multiplicative Error Model which combines the mixed frequency features of a MIDAS with Markovian dynamics. When estimated in–sample on the realized kernel volatility of the S&P500 index, this model dominates other simpler specifications, especially when monthly aggregated realized volatility is used. The same pattern is confirmed in the out–of–sample forecasting performance which suggests that adding an abrupt change in the average level of volatility better helps in tracking extreme episodes of volatility and a relative quick absorption of the shocks.

Keywords: Realized Volatility, Multiplicative Error Model, Markov switching, MIDAS, Short– and Long–Run Components
Jel Classification: C22, C24, C38, C58.

[*] Department of Statistics, Computer Science, Applications; E-mail: luca.scaffididomianello@unifi.it
[±] E-mail: giampiero.gallo@nyu.edu
[∝] Corresponding author - Department of Economics; E-mail: eotranto@unime.it

1 Introduction

Recurrent global economic and financial crises have prompted an interest in studying the interdependence between the real economy and the financial market volatility. Starting from Officer (1973) and Schwert (1989), several authors document the economic sources of volatility and, in particular, its increase during a recession while reverting to more physiological states during expansion phases (the so–called *countercyclical* pattern of stock market volatility). In an attempt to bring together economic factors (typically measured at a low frequency) within a financial framework (whose status is observable at a much higher frequency), Engle et al. (2013) provided a pathbreaking perspective within this strand of literature by introducing the GARCH-MIDAS model, a multiplicative component model in which the conditional variance is decomposed into short– and long–run components. Component models, introduced by Engle and Lee (1999), can capture the volatility dynamics putting together a parsimonious structure containing a slow–moving, more persistent component and a shorter-lived one. In the case of the GARCH-MIDAS, the short–run component follows a GARCH–type dynamics aimed at capturing volatility clustering and daily fluctuations, while the long-run one represents a time–varying average level of volatility, driven by macroeconomic and/or financial variables. A distinctive merit of this class of models is to be able to mix different frequencies of observability within the same analysis.

Volatility modeling within the GARCH framework is based on the daily squared returns, a noisy, albeit unbiased, measure of conditional variance. A big boost to studying the dynamics of volatility is provided by the availability of ultra-high frequency data, which allows for more precise volatility measures in the wide class of Realized Volatility (RV) Andersen et al. (2003): from the plain vanilla version of RV, as the sum of squared high-frequency returns (sampled at, e.g., five minutes), more refined versions taking into consideration autocorrelation of intradaily returns or microstructure noise, such as the Realized kernel volatility of Barndorff-Nielsen et al. (2008) are available as more robust estimators of volatility. Following Andersen and Bollerslev (1998), it is now customary to use such a variable as the suitable target to evaluate forecast performance of volatility models.

Apart from being a consistent measure of ex-post daily volatility, RV lends itself to being modeled for forecasting purposes, given its empirical features of long–run dependence and volatility clustering: being a positive–valued process, new models such as the Multiplicative Error Model (MEM, Engle, 2002; Engle and Gallo, 2006) have proved useful to reproduce its dynamics. Some component extension of the MEM are present in the literature (see, e.g., the Composite MEM of Brownlees et al., 2012), while Amendola et al. (2021) proposed the MEM-MIDAS to exploit the relationship between economics and financial volatility by focusing on the RV as the variable of interest, *in lieu* of the squared returns as in the GARCH-MIDAS.

While the modelling effort provides some interesting insights on the interpretability of the long–run component of volatility responding to economic factors, the MEM-MIDAS model is not able to capture abrupt shifts in the average level of volatility, which are typical of sudden crises and panic behavior on the financial markets, accompanying a change in the short–run dynamics (i.e. more sensitivity to recent news). To this end, in this paper[1] we add a Markov Switching (MS) dynamics to the short– and long–run

[1] This paper is an extended version of the work presented at the 51st Scientific Meeting of the Italian Statistical Society on June, 2022 (Balzanella et al., 2022).

component to the MEM–MIDAS: the resulting model is the MS-MEM-MIDAS[2]. Given that MS models can be seen as an alternative approach to capture a changing level of average volatility (long–run component reacts across regimes with a step function and then remains constant within each regime), the model allows for an insight of which component provides a better fit to the actual slow–moving behavior of observed volatility, whether the contribution of economic variables observed at a lower frequency, or the Markov switching component (with its sudden adjustment of the average level of volatility), or, yet, a combination of both.[3] From what emerges in our empirical application, conducted on the realized kernel volatility of the S&P500 index, the MS-MEM-MIDAS offers improvements both in– and out–of–sample relative to a Markov Switching MEM (without the MIDAS component) and to a MEM-MIDAS without switching behavior.

The paper is organized as follows: Section 2 describes the new model proposed, Section 3 analyzes the finite sample properties of the estimator through a Monte Carlo simulation, and Section 4 illustrates the empirical analysis, with some concluding remarks following.

2 A New Model in the MEM Class

The MEM[4] is a class of time series models for non–negative processes $\{x_t\}$ describing the evolution of phenomena related to financial market activity (e.g. volatility, durations Engle and Russell, 1998, volumes Manganelli, 2005, number of trades, etc.) that, in its asymmetric structure, is specified as follows:

$$\begin{aligned}
&x_t = g_t \tau \epsilon_t, \\
&\epsilon_t \sim \text{Gamma}\left(a_1, 1/a_1\right) \quad \forall t \\
&g_t = (1-\alpha_1-\beta_1-\gamma_1/2) + \alpha_1 \frac{x_{t-1}}{\tau} + \beta_1 g_{t-1} + \gamma_1 D_{(r_{t-1}<0)} \frac{x_{t-1}}{\tau}.
\end{aligned} \tag{1}$$

The specification in Eq. (1) implies that $\mu_t = g_t \tau$ is the expectation of x_t, conditional on the information set at the previous period, $\mathcal{I}_{t-1}$, i.e. $E\left(x_t | \mathcal{I}_{t-1}\right) = \mu_t$, given that the error term ϵ_t follows a Gamma distribution with a unit mean.[5] D is a dummy variable equal to 1 when the returns at time t is negative, 0 otherwise, and the coefficient γ_1 captures the so–called leverage effect, whereby a negative return impacts subsequent volatility more than a positive one. Moreover, to ensure the positiveness and the stationarity of the process, we apply the usual sufficient constraints: $\alpha_1 \geq 0$, $\beta_1 \geq 0$, $\gamma_1 \geq 0$ and $\alpha_1 + \beta_1 + \gamma_1/2 < 1$. Under the given stationarity, the unconditional mean is equal to τ.

In order to accommodate variables observed at different frequencies, let us now define a double time index for the variable of interest. With a slight abuse of notation, let $\{x_{i,t}\}$ be the same non–negative process, where now we isolate the i-th day within the

[2]The model by Pan et al. (2017) adopts a simplified MS setup for the constant term in a GARCH–MIDAS framework.

[3]This idea of combining MS dynamics with some smooth component is at the basis of the *fuzzy* approach by Gallo and Otranto (2018).

[4]For a recent paper which offers a perspective of the evolution of MEM modeling in the presence of low– and high–frequency components see Cipollini and Gallo (2022).

[5]In order to ensure the non–negativeness of x_t the error term is defined on a positive support. Parameters are identified by a 1 subscript in order to allow the comparison with other models presented below.

low-frequency period t (be it a week, a month, or a quarter). The relevant conditioning set becomes then $\mathcal{I}_{i-1,t}$.

The MEM-MIDAS is specified as a multiplicative component model:

$$
\begin{aligned}
& x_{i,t} = g_{i,t}\tau_t\epsilon_{i,t} \\
& \epsilon_{i,t} \sim Gamma\,(a, 1/a) \quad \forall\ i = 1, ..., N_t \quad \text{and} \quad t = 1, ..., T \\
& g_{i,t} = (1-\alpha_1-\beta_1-\gamma_1/2) + \alpha_1\frac{x_{i-1,t}}{\tau_t} + \beta_1 g_{i-1,t} + \gamma_1 D_{(r_{i-1,t}<0)}\frac{x_{i-1,t}}{\tau_t} \\
& \tau_t = exp\left\{\omega_1 + \theta\sum_{k=1}^{K}\varphi_k(\lambda_1,\lambda_2)X_{t-k}\right\} \\
& \varphi_k(\lambda_1,\lambda_2) = \frac{(k/K)^{\lambda_1-1}(1-k/K)^{\lambda_2-1}}{\sum_{j=1}^{K}(j/K)^{\lambda_1-1}(1-j/K)^{\lambda_2-1}}
\end{aligned}
\tag{2}
$$

where $g_{i,t}$, the short-run component,[6] follows a unit mean MEM process and τ_t is a slow-moving component driven by a low frequency stationary variable, X_t, where the exponential form is used to ensure its positiveness. The MIDAS filter is based on $\varphi_k(\lambda_1,\lambda_2)$, a weighting function of the past K values of X_t, with weights summing up to one. This filter, based on the beta function, is quite flexible, allowing us to link variables sampled at a different frequency. We set $\lambda_1 = 1$ and $\lambda_2 > 1$, to ensure a monotonically decreasing pattern, as far as λ_2 increases, that is the most recent observations have more influence on the long-run component.

In order to allow for an abrupt shift in the average level of volatility, we suggest the novel MS MEM-MIDAS as a multiplicative model with several components in the presence of a Markovian dynamics:[7]

$$
\begin{aligned}
& x_{i,t} = g_{i,t,s_{i,t}}\tau_{i,t}\epsilon_{i,t} \\
& \epsilon_{i,t}|s_{i,t} \sim Gamma\left(a_{s_{i,t}}, 1/a_{s_{i,t}}\right) \quad \forall\ i = 1, ..., N_t \quad \textit{and} \quad t = 1, ..., T \\
& g_{i,t,s_{i,t}} = (1-\alpha_{s_{i,t}}-\beta_{s_{i,t}}-\gamma_{s_{i,t}}/2) + \alpha_{s_{i,t}}\frac{x_{i-1,t}}{\tau_{i-1,t}} + \\
& + \beta_{s_{i,t}} g_{i-1,t,s_{i-1,t}} + \gamma_{s_{i,t}} D_{(r_{i-1,t}<0)}\frac{x_{i-1,t}}{\tau_{i-1,t}} \\
& \tau_{i,t} = exp\left\{\omega_{s_{i,t}} + \theta\sum_{k=1}^{K}\varphi_k(\lambda_1,\lambda_2)X_{t-k}\right\} \\
& \varphi_k(\lambda_1,\lambda_2) = \frac{(k/K)^{\lambda_1-1}(1-k/K)^{\lambda_2-1}}{\sum_{j=1}^{K}(j/K)^{\lambda_1-1}(1-j/K)^{\lambda_2-1}}.
\end{aligned}
\tag{3}
$$

In this specification, coefficients in the short–run component depend on a regime represented by a discrete time latent variable, $s_{i,t}$, which varies as a first–order Markov chain at the higher frequency according to transition probabilities:

$$
P\{s_{i,t} = j|s_{i-1,t} = l\} = p_{lj} \quad \forall\ l, j = 1, \ldots, J, \tag{4}
$$

with p_{lj} the transition probability and J the number of states (with the usual constraints). In this model, also the low–frequency component is allowed to change within period t according to a constant $\omega_{s_{i,t}}$ which changes with the same regimes.

The estimation of the parameter of the MS MEM–MIDAS can be obtained through the Quasi Maximum Likelihood Estimator (QMLE). The log-likelihood is a by-product

[6] Notice that when $i = 1$, then $(i-1, t) = (N_{t-1}, t-1)$.

[7] See Gallo and Otranto (2015) for a comprehensive description of the MS MEM.

of the Hamilton filter[8] and it is specified as follows:

$$
\begin{aligned}
&LL = \sum_{t=1}^{T}\sum_{i=1}^{N_t} ll_{i,t} = \sum_{t=1}^{T}\sum_{i=1}^{N_t} log f(x_{i,t}|\mathcal{I}_{i-1,t}) \\
&f(x_{i,t}|\mathcal{I}_{i-1,t}) = \sum_{s_{i,t}}\sum_{s_{i-1,t}} f(x_{i,t}|\mathcal{I}_{i-1,t}, s_{i,t}, s_{i-1,t})P(s_{i,t}, s_{i-1,t}|\mathcal{I}_{i-1,t}) \\
&f(x_{i,t}|\mathcal{I}_{i-1,t}, s_{i,t}, s_{i-1,t}) = \frac{a_{s_{i,t}}^{a_{s_{i,t}}}\ \mu_{i,t,s_{i,t}}^{-a_{s_{i,t}}}\ x_{i,t}^{(a_{s_{i,t}}-1)} \exp\left(-a_{s_{i,t}}\dfrac{x_{i,t}}{\mu_{i,t,s_{i,t}}}\right)}{\Gamma(a_{s_{i,t}})}
\end{aligned}
\tag{5}
$$

where $\Gamma(\cdot)$ is the gamma function. In order to complete the log-likelihood function, then, we need the predicted probabilities, $P(s_{i,t}, s_{i-1,t}|\mathcal{I}_{i-1,t})$, which are obtained, as part of the Hamilton filter, by iterating the following equations:

$$
\begin{aligned}
&P(s_{i,t}, s_{i-1,t}|\mathcal{I}_{i-1,t}) = P(s_{i,t}|s_{i-1,t})P(s_{i-1,t}|\mathcal{I}_{i-1,t}) \\
&P(s_{i,t}, s_{i-1,t}|\mathcal{I}_{i,t}) = \frac{f(x_{i,t}|\mathcal{I}_{i-1,t}, s_{i,t}, s_{i-1,t})P(s_{i,t}, s_{i-1,t}|\mathcal{I}_{i-1,t})}{\sum_{s_{i,t}}\sum_{s_{i-1,t}} f(x_{i,t}|\mathcal{I}_{i-1,t}, s_{i,t}, s_{i-1,t})P(s_{i,t}, s_{i-1,t}|\mathcal{I}_{i-1,t})}
\end{aligned}
\tag{6}
$$

with $P(s_{i,t}|\mathcal{I}_{i,t}) = \sum_{s_{i-1,t}} P(s_{i,t}, s_{i-1,t}|\mathcal{I}_{i,t})$.[9]

In this setup, the conditional volatility, $\mu_{i,t,s_{i,t}}$, suffers from the so–called path dependence problem, that is, it depends on the whole history of the latent variable $s_{i,t}$. To circumvent that, we use the following collapsing procedure at each step of the Hamilton filter adopted by Gallo and Otranto (2015), based on Kim (1994):

$$
\hat{\mu}_{i,t,s_{i,t}} = \frac{\sum_{s_{i-1,t}} P\{s_{i,t}, s_{i-1,t}|\mathcal{I}_{i,t}\}\hat{\mu}_{i,t,s_{i,t},s_{i-1,t}}}{P\{s_{i,t}|\mathcal{I}_{i,t}\}}, \tag{7}
$$

i.e. by averaging the J^2 possible values of the conditional volatility $\mu_{i,t,s_{i,t}}$, with the weights equal to the corresponding filtered probabilities.

Due to the latent nature of the variable $s_{i,t}$, we can only make inference on which regime the process was for each day, based on the sample information. So, if we use the full sample information, the inference about regime is called smoothed probability, that is we need to calculate $P(s_{i,t}|\mathcal{I}_{N_T,T})$. It is obtained for each date through the Kim's algorithm (see, again, Kim, 1994):

$$
P(s_{i,t}, s_{i+1,T}|\mathcal{I}_{N_T,T}) = \frac{P(s_{i+1,t}|s_{i,t})P(s_{i,t}|\mathcal{I}_{i,t})P(s_{i+1,t}|\mathcal{I}_{N_T,T})}{P(s_{i+1,t}|\mathcal{I}_{i,t})} \tag{8}
$$

with $P(s_{i,t}|\mathcal{I}_{N_T,T}) = \sum_{s_{i+1,t}} P(s_{i,t}, s_{i+1,t}|\mathcal{I}_{N_T,T})$. Then, by iterating eq. (8) for $t = (N_T, T), (N_T-1, T)\dots(1, T), (N_{T-1}, T-1)\dots(1, 1)$, we get the smoothed probability. All we need to start Kim's algorithm is $P(s_{N_T,T}|\mathcal{I}_{N_T,T})$, obtained at the last iteration of the Hamilton filter.

Such an estimator is interpretable as a Quasi Maximum Likelihood Estimator and, as such, possesses the properties of consistency and asymptotic normality: Bollerslev and Wooldridge (1992) is the main reference for the study of these properties in dynamic models that jointly parameterize conditional means and conditional covariances, adopting the normal density to generate the likelihood function when this hypothesis is not

[8] See Hamilton (1994), chapter 22, for the technical details about the Hamilton filter.

[9] To start the filter we need $P(s_{0,0})$, then we use as starting values the unconditional probabilities (see Hamilton, 1994).

valid. The classical asymptotic results and properties of QMLE have been extended to the GARCH–MIDAS model, under a set of assumptions, by Wang and Ghysels (2015). QMLE properties of MEMs and MS models were investigated by Engle and Gallo (2006) and Kim, 1994 respectively. Similarly, Amendola et al. (2021) derive QMLE and standard errors for MEM–MIDAS.

3 A Monte Carlo Investigation

The finite sample properties of QMLE, even when models are extensions and combinations of previous established models, are better investigated by means of Monte Carlo experiments: Conrad and Kleen (2020) verified the results of Wang and Ghysels (2015);Amendola et al. (2019) study the QMLE properties of their asymmetric GARCH–MIDAS; Gallo and Otranto (2015) analyze their MS–MEM.

For our MS–MEM–MIDAS, we calculate the mean and the standard deviations of the QML estimates obtained on simulated data with increasing sample size to verify consistency, and we apply the Kolmogorov nonparametric test (Kolmogorov, 1933) to verify the normality of the sampling distributions.

Our Monte Carlo experiment consists of generating series from model in eq. (3)[10] with length $T = \{1500, 2100, 2700, 3300, 9900\}$; the number of replications is 600. To consider plausible and realistic parameters of the data generating process, we adopt the values obtained in the empirical analysis.[11] The low frequency variable follows an AR(4) process, i.e., $X_t = \sum_{i=1}^{4} \phi_i X_{t-i} + u_t,\ u_t \sim N(0, \sigma_u)$, while the daily return an AR(2) process, $r_t = \sum_{i=1}^{2} \psi_i r_{t-i} + \xi_t,\ \xi_t \sim N(0, \sigma_\xi)$.[12] The number of days, N_t for each month is set equal to 30 $\forall\, t$ (a simplification without practical consequences), while the number of lags, K, in the MIDAS filter involving the low frequency variable is equal to 36, both in the data generation and in the estimation.

The main characteristics of the QMLE are shown in Table 1 and can be synthesized as follows:

- the means of estimated parameters in the simulations suggest unbiasedness of the estimators $\hat{\beta}_1$, $\hat{\gamma}_1$ and $\hat{\theta}$ even in small samples. Most of the other estimators reach the true value for larger sample sizes;
- in other cases, the estimators of the constants ω_1 and ω_2 and of the parameters of the Gamma density a_1 and a_2 show a small bias, which remains also for larger T's. Similar results were encountered by Gallo and Otranto (2015) in analyzing the properties of the MS–AMEM;
- generally the root mean squared error of the estimators decreases as the length of the series increases, suggesting asymptotic efficiency;

[10] To speed up the estimation procedure, we consider 2 regimes and only the constant and the parameter related to the Gamma density as switching coefficients.

[11] For the sake of brevity, we did not report the estimate results for the MS(2) MEM MIDAS, but they are available on request.

[12] The parameters of the low frequency variable are obtained by fitting an AR(4) to the IP growth rate, and are equal to 0.06, 0.17, 0.24 and 0.22 for the first, second, third and fourth lag respectively. Whereas the parameters, relative to the returns, are obtaind by fitting an AR(2) to their series and are equal to -0.1 and -0.6 for the first and second lag, respectively.

- the results are coherent with asymptotic normality of the estimators. The only exceptions appear when estimating the transition probabilities p_{11} and p_{22}; a plausible justification for this is that the true value of these parameters is close to the upper bound of the coefficients, forcing a negative skewness in the empirical distribution.

These results are supported by a visual inspection of the empirical distributions of the estimated parameters across replications (when $T = 9900$), shown in Figure 1, where the estimates are standardized using the true parameter as the mean, and contrasted against a standard Normal density profile. In particular, the slight positive bias in the estimated intercepts $\hat{\omega}_1$ and $\hat{\omega}_2$ and the negative asymmetry of the estimated transition probabilities $\hat{p}_{11}$ and $\hat{p}_{22}$ are confirmed.

4 Empirical Analysis

We select as dependent variable the S&P 500 annualized Realized kernel volatility[13] (RV); for comparison purposes, we choose three different low frequency variables: the industrial production (IP) growth rate, the monthly RV, and the Equity Market Volatility (EMV) indicator for Macroeconomics News and Outlook of Baker et al. (2019).[14]

Overall, we estimate 8 models: the MEM, MS(3) MEM, the MEM-MIDAS and three MS(3)-MEM-MIDAS each for the three low frequency variables indicated above. The results for the first estimation period between January 2, 2003 and December 31, 2014, are presented in Table 2.

The estimated parameters are in line with the previous studies mentioned: the coefficient θ (which translates the MIDAS filter of the low–frequency variable on the high–frequency one) is negative when the forcing variable of the long–run component is the IP growth rate, the known *countercyclical* pattern of volatility, while it is positive when we consider the monthly RV or the EMV tracker. In addition, the value of λ_2 (which commands the way in which the most recent observations of the low–frequency X_t impact the long–run component) is quite high, giving more weight to the recent past, especially when the financial variables are used.

We consider three regimes in the Markov Switching models (as Gallo and Otranto (2015) do), so that we are able to discriminate across low–, mid–, and high–volatility periods. We note that the α_2 coefficient is practically zero for all MS models, whereas the γ_2 is significant, showing that the volatility dynamics in the mid–volatility regime is affected by just negative news. Recalling that the variance of the Gamma distribution with a single parameter is equal to $1/a_{s_t}$, the mid–volatility regime is accommodating a disturbance with the smallest variance. Among the models, a peculiar behavior is exhibited by the MS(3) MEM-MIDAS-RV, where the variance of the high–volatility regime is twice the variance of the mid–volatility regime, and this is accompanied by a larger number of observations assigned to the third regime relative to what other MS models do.

[13] The realized variance taken from Oxford-Man Institute's Realized Library (https://realized.oxford-man.ox.ac.uk/data/download) is multiplied by the conventional 252 to express it in annualized terms. For our purposes, we consider the percent realized volatility as its square root times 100. It is well known that the realized volatility in general is subject to a measurement error Bollerslev et al. (2016); Cipollini et al. (2021) show that the MS–MEM class is a way to introduce robustness to measurement errors in modeling volatility dynamics.

[14] The data for IP and EMV are available at https://fred.stlouisfed.org/series, while monthly RV is the aggregation of the daily RV for each month.

Table 1: Monte Carlo simulation of 600 series with different length $T = \{1500, 2100, 2700, 3300, 9900\}$. For the Data Generating Process see eq. (3).

	True	T=1500			T=2100			T=2700			T=3300			T=9900		
		Average	RMSE	Normality	Average	RMSE	Normality	Average	RMSE	Normality	Average	RMSE	Normality	Average	RMSE	Normality
α_1	0.051	0.046	0.015	0.356	0.049	0.012	0.511	0.048	0.01	0.493	0.050	0.009	0.918	0.051	0.005	0.787
β_1	0.836	0.839	0.017	0.699	0.837	0.013	0.989	0.838	0.011	0.255	0.836	0.011	0.955	0.835	0.006	0.82
γ_1	0.124	0.125	0.009	0.924	0.125	0.008	0.816	0.125	0.007	0.923	0.124	0.006	0.753	0.125	0.004	0.958
ω_1	0.585	0.606	0.074	0.022	0.599	0.062	0.073	0.597	0.055	0.973	0.602	0.049	0.529	0.598	0.03	0.164
ω_2	1.677	1.778	0.242	0.032	1.769	0.215	0.000	1.757	0.168	0.322	1.756	0.151	0.293	1.722	0.088	0.884
a_1	7.677	7.732	0.256	0.463	7.712	0.219	0.853	7.689	0.187	0.999	7.673	0.162	0.999	7.666	0.098	0.587
a_2	7.990	8.321	0.992	0.000	8.154	0.781	0.000	8.026	0.631	0.357	8.064	0.577	0.019	7.950	0.296	0.129
θ	-0.177	-0.177	0.009	0.892	-0.177	0.007	0.827	-0.177	0.006	0.767	-0.177	0.006	0.304	-0.177	0.003	0.978
p_{11}	0.994	0.992	0.003	0.000	0.993	0.003	0.000	0.993	0.002	0.011	0.993	0.002	0.087	0.994	0.001	0.048
p_{22}	0.956	0.942	0.026	0.000	0.946	0.022	0.000	0.949	0.017	0.000	0.951	0.015	0.000	0.955	0.007	0.030

Average estimates, root mean squared error and p-value of the Kolmogorov Smirnov test to test the null hypothesis of normality of the parameters sampling distribution for the Monte Carlo exercise. λ_2 has a RMSE equal to 0, then it follows a degenerating distribution. To speed up the estimation procedure, we consider two regimes and the constant and the parameter related to the Gamma density as switching coefficients. The long run variable is assumed to follow an AR(4) process, $X_t = \phi_1 X_{t-1} + \phi_2 X_{t-2} + \phi_3 X_{t-3} + \phi_4 X_{t-4} + u_t,\ u_t \sim N(0, \sigma_u)$, while the daily return an AR(2) process, $r_t = \psi_1 r_{t-1} + \psi_2 r_{t-2} + \xi_t,\ \xi_t \sim N(0, \sigma_\xi)$. The number of days, N_t for each month is equal to 30, while the number of lags, K, of the low frequency variable is equal to 36.

Figure 1: Standardized empirical distributions of parameter estimates relative to the true value for 600 MC replications of length $T = 9900$. The density of the standard normal distribution is superimposed as a continuous line.

(a) $\hat{\alpha}_1$

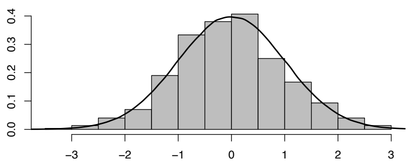

(b) $\hat{\beta}_1$

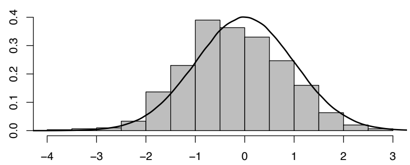

(c) $\hat{\gamma}_1$

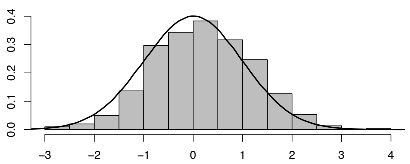

(d) $\hat{\omega}_1$

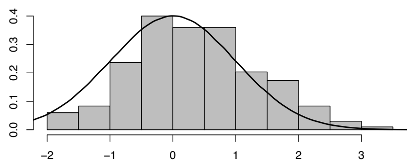

(e) $\hat{\omega}_2$

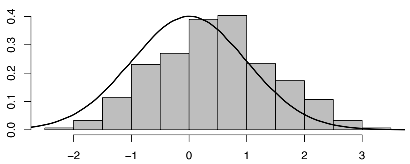

(f) $\hat{a}_1$

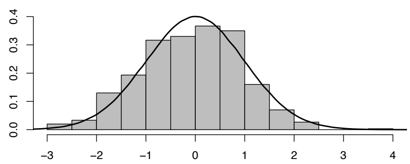

(g) $\hat{a}_2$

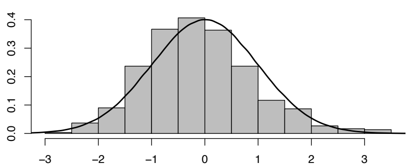

(h) $\hat{\theta}$

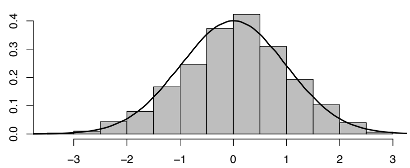

(i) $\hat{p}_{11}$

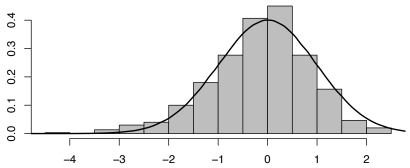

(j) $\hat{p}_{22}$

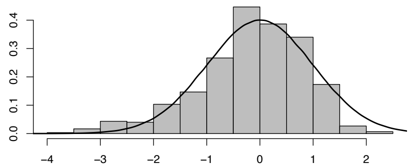

Table 2: Parameter estimated (Jan. 2, 2003 – Dec. 31, 2014) with standard errors in parentheses for annualized realized kernel volatility.

	MEM[1]	MEM MIDAS IP	MEM MIDAS EMV	MEM MIDAS RV	MS(3) MEM	MS(3) MEM MIDAS IP	MS(3) MEM MIDAS EMV	MS(3) MEM MIDAS RV
α_1	0.119	0.107	0.094	0.096	0.041	0.038	0.044	0.027
	(0.016)	(0.016)	(0.015)	(0.015)	(0.023)	(0.016)	(0.014)	(0.019)
β_1	0.768	0.769	0.750	0.751	0.768	0.775	0.789	0.774
	(0.017)	(0.017)	(0.017)	(0.017)	(0.042)	(0.029)	(0.023)	(0.066)
γ_1	0.128	0.135	0.147	0.149	0.164	0.164	0.157	0.166
	(0.012)	(0.012)	(0.012)	(0.012)	(0.020)	(0.019)	(0.014)	(0.034)
α_2					0.000	0.000	0.000	0.000
					(0.000)	(0.000)	(0.000)	(0.000)
β_2					0.843	0.832	0.733	0.880
					(0.033)	(0.031)	(0.184)	(0.036)
γ_2					0.103	0.101	0.045	0.054
					(0.034)	(0.027)	(0.047)	(0.057)
α_3					0.155	0.051	0.054	0.181
					(0.040)	(0.039)	(0.165)	(0.081)
β_3					0.724	0.800	0.690	0.673
					(0.048)	(0.040)	(0.242)	(0.073)
γ_3					0.117	0.171	0.240	0.156
					(0.033)	(0.032)	(0.054)	(0.037)
ω_1	2.518	2.578	1.403	1.867	2.219	2.364	1.418	1.815
	(0.036)	(0.031)	(0.079)	(0.050)	(0.042)	(0.029)	(0.076)	(0.047)
ω_2					2.627	2.763	1.744	2.060
					(0.087)	(0.042)	(0.101)	(0.141)
ω_3					3.157	3.366	2.330	2.367
					(0.148)	(0.072)	(0.113)	(0.127)
a_1	6.874	7.020	7.203	7.196	7.655	7.540	7.488	7.568
	(0.276)	(0.244)	(0.202)	(0.201)	(0.305)	(0.235)	(0.210)	(0.344)
a_2					8.018	9.318	10.84	11.97
					(1.075)	(0.744)	(1.476)	(2.699)
a_3					8.012	7.456	7.695	6.436
					(0.728)	(0.644)	(1.065)	(0.800)
θ		-0.223	0.074	0.045		-0.207	0.066	0.038
		(0.051)	(0.005)	(0.003)		(0.019)	(0.005)	(0.004)
λ_2		2.691	5.824	9.934		2.770	4.490	7.610
		(1.850)	(1.102)	(1.737)		(0.352)	(0.742)	(2.676)
p_{11}					0.994	0.996	0.995	0.997
					(0.004)	(0.002)	(0.002)	(0.002)
p_{22}					0.973	0.977	0.956	0.968
					(0.010)	(0.009)	(0.017)	(0.017)
p_{33}					0.987	0.971	0.972	0.983
					(0.006)	(0.011)	(0.018)	(0.017)
p_{12}					0.006	0.004	0.005	0.001
					(0.004)	(0.002)	(0.002)	(0.004)
p_{21}					0.016	0.012	0.033	0.015
					(0.009)	(0.007)	(0.015)	(0.013)
p_{32}[2]					0.013	0.029	0.028	0.017
					(0.007)	(0.011)	(0.018)	(0.017)
LogLik	-8611.61	-8578.42	-8537.78	-8539.33	-8509.89	-8489.82	-8483.89	-8477.97

[a]To facilitate the comparison with the parameters of the other models, we reparameterize τ in Eq. (1) with $exp(\omega_1)$.

[b]The elements of the transition probability matrix p_{13}, p_{23}, p_{31} can be derived as the complement to one of the sum of the other elements by row.

In Figure 2, we translate the largest value of the smoothed probabilities into an inference on the regimes by assigning each observation to the corresponding state. In general, all MS models are able to capture the correspondence between the severe market downturn periods and the high–volatility regime: the bankruptcy of Lehman Brothers in September 2008, the flash crash in May 2010 (with the exception of the MS(3) MEM-MIDAS-EMV) and the credit rating downgrade of the United States sovereign debt in the second half of the year 2011. The MS(3) MEM-MIDAS-RV seems to have better classification capabilities, as it assigns the subprime mortgage crisis period (second half 2007-first half 2009) to the high-volatility regime (green points), while other MS(3) MEM-MIDAS models manage to assign to the third regime just the main peaks. By the same token, the MS(3) MEM-MIDAS-EMV seems to be the least reactive model, favoring the assignment of most observations to the low–volatility regime, and missing some notable burst of volatility, especially toward the end of 2007.

The visual inspection of the dynamics across regimes shown in Figure 2, can be further analyzed calculating the average duration in each regime i as $1/(1-p_{ii})$ (Hamilton, 1994). For the models at hand the differences in the persistence within each of the three regimes can be appreciated from Table 3; the low–volatility period is the most persistent one (more than 200 days using the MS(3) MIDAS models, and even longer when RV is used as the low–frequency variable). By the same token, both Regime 2 and 3 are considerably shorter with durations in either state between approximately 30 and 60 days: this is consistent with the idea that the switches in volatility, be they moderate increases or extreme bursts, are relatively short–lived.

The similarities and the differences among the inferences on the regimes derived from the four MS models can be better appreciated by looking at Table 4, where we show the percentage frequencies of the observations conditional on the regime i ($i = 1, 2, 3$) in the model by row falling in the regime j ($j = 1, 2, 3$) for the model by column. On the diagonal of each sub–block we have the degree of agreement of what is classified by the model in the row with the corresponding classification by the model in the column. By and large, there is a high level of agreement in what concerns the first regime, with the exception of the mixed–frequency model involving the variable EMV. In terms of the second regime, the degree of concordance substantially decreases (with one exception: 92% of the observations classified in the second regime in the mixed model with RV belong to the same regime with the IP model). For the third regime, the agreement is at times high but one can notice an asymmetry in the relationship in that, for example, all observations classified as regime 3 by the EMV mixed model belong to the third regime when the mixed model uses IP, but the reverse is not true: only 48% of the observations classified in Regime 3 by the IP mixed model fall in the same regime in the EMV mixed model. Other cases share the same asymmetric pattern.

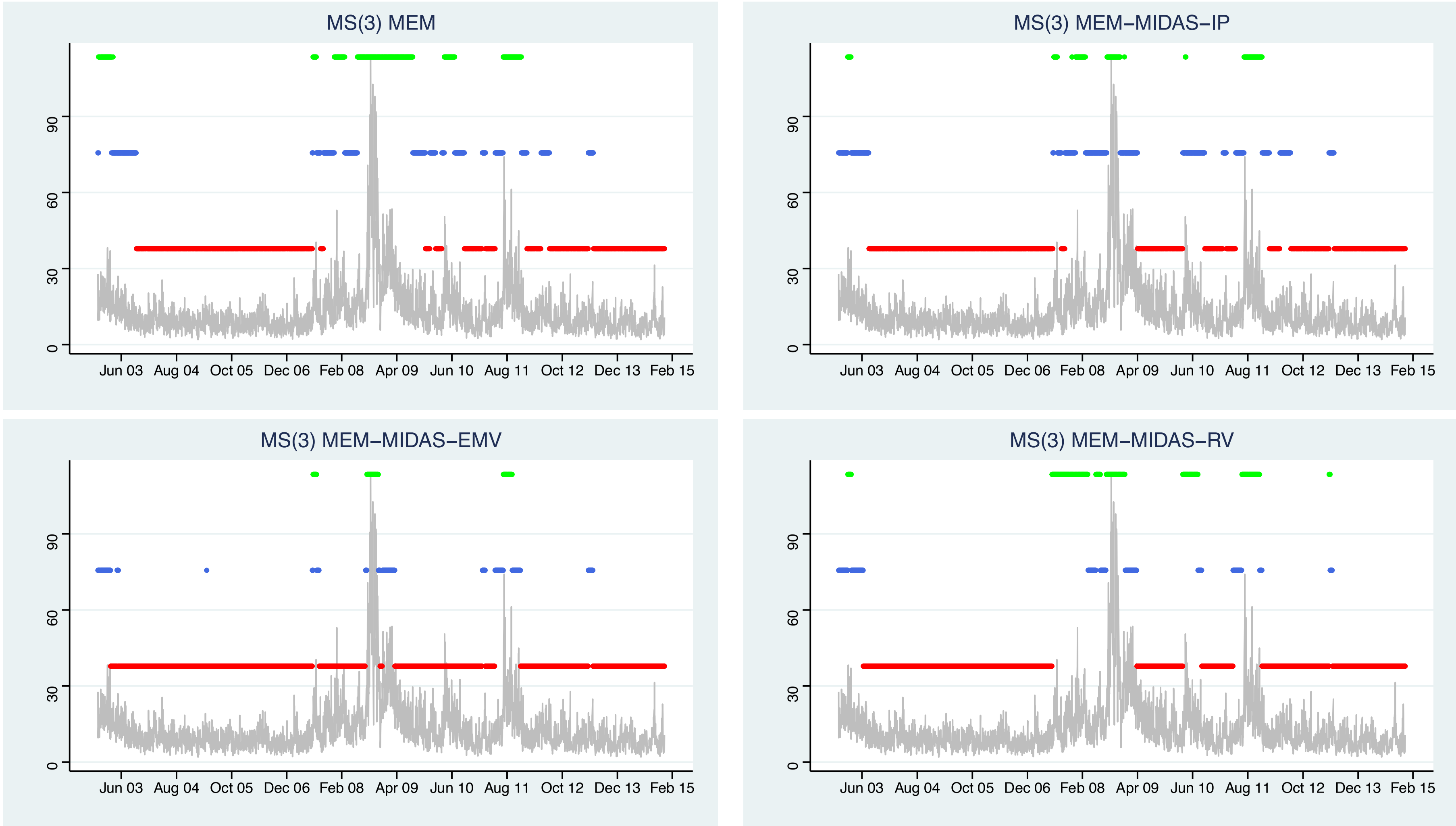

Figure 2: Smoothed inference of four models and annualized realized kernel volatility (gray line). The observations are assigned to a volatility regime based on the value of the smoothed probabilities. Low–volatility regime (red points), mid–volatility regime (blue points) and high–volatility regime (green points). Sample: Jan. 2, 2003 – Dec. 31, 2014.

Table 3: Average duration, expressed as number of days, in each regime for the MS models. Sample: Jan. 2, 2003 – Dec. 31, 2014.

	MS(3) MEM	MS(3) MEM MIDAS IP	MS(3) MEM MIDAS EMV	MS(3) MEM MIDAS RV
Regime 1 (s_1)	177	224	208	354
Regime 2 (s_2)	37	44	23	31
Regime 3 (s_3)	78	35	36	58

The average duration in days within each regime s_i with $i = 1, 2, 3$ is calculated as $1/(1 - p_{ii})$.

Table 4: Frequency table of inference on regimes of four models. Sample: Jan. 2, 2003 – Dec. 31, 2014.

		MS(3) MEM			MS(3) MEM MIDAS IP			MS(3) MEM MIDAS EMV			MS(3) MEM MIDAS RV		
		s_1	s_2	s_3	s_1	s_2	s_3	s_1	s_2	s_3	s_1	s_2	s_3
MS(3) MEM	s_1				98.7	1.3	0.0	99.9	0.1	0.0	98.0	0.8	1.2
	s_2				24.5	75.0	0.5	81.7	18.1	0.2	48.1	27.1	24.8
	s_3				14.5	41.1	44.4	46.0	32.3	21.7	15.3	26.4	58.2
MS(3) MEM MIDAS IP	s_1	88.3	7.4	4.3				100.0	0.0	0.0	98.1	0.7	1.2
	s_2	3.2	63.3	33.6				68.5	31.5	0.0	24.1	42.8	33.1
	s_3	0.0	1.1	98.9				23.2	28.1	48.7	0.4	4.9	94.8
MS(3) MEM MIDAS EMV	s_1	70.0	19.4	10.6	78.3	19.3	2.4				82.7	6.8	10.5
	s_2	0.7	36.4	63.0	0.3	75.1	24.6				8.2	53.4	38.4
	s_3	0.0	0.8	99.2	0.0	0.0	100.0				0.0	0.0	100.0
MS(3) MEM MIDAS RV	s_1	82.1	13.7	4.2	91.8	8.1	0.0	98.8	1.2	0.0			
	s_2	4.4	49.1	46.4	4.1	92.0	3.8	51.8	48.2	0.0			
	s_3	4.0	29.3	66.7	4.8	46.4	48.7	52.4	22.5	25.0			

Each value represent the percent frequency of the inferred regime of the model by column conditionally on the inferred regime of the model by row. The observations are assigned to a volatility regime (s_i with $i = 1, 2, 3$) based on the value of the smoothed probabilities.

The overall behavior in comparing the classification of the regimes can be appreciated graphically in Figure 3, where we consider the models two at a time (six panels total), and we build stacked bars differentiated by color according to whether the classification is common to both models (light blue - hence the same height of this bar by panel) or specific (blue - on top of the previous one). This graph allows us first to appreciate how many observations are allocated to each regime by individual models (all panels share the same vertical scale), and to identify the model that has the highest overall bar. In this respect across models, the EMV mixed model tends to favor Regime 1 (2581 over 3016 observations), while the IP mixed model has the highest number of observations (729) classified as Regime 2 and, finally, the MS(3) MEM, which does not make use of the smooth trend, has 594 observations allocated to Regime 3. While the height of the bar does not change across comparisons, its composition does and hence one may find a different allocation of observations between those that are common to both models and those that are specific. The second comparison, then is one in which we evaluate similarity (or differences) across models and regimes by noting how similar (or different) the total height is and how small the darker blue portion of the bar. Hence, for example, for Regime 3, the MS(3) MEM and the RV mixed model (M1 vs M4) give similar overall results, while one notices that each model contributes a substantial portion of the specific classification (same is true for M1 vs M2 or M3 vs M4 in Regime 2).

By calculating an adjusted Rand index Hubert and Arabie (1985) and Rand (1971) for group similarity, the highest value is encountered for the pair of mixed models with IP and RV, respectively (0.84); the same IP model ranks next with the MS(3) MEM (0.79). The lowest value of the index (0.63) is reached by the pair MS(3) MEM with the EMV mixed model, which, in general, differs in terms of its classification capabilities.

Figure 3: Pairwise comparison of inferred regimes among four MS models.
M1: MS(3)MEM; **M2**: MS(3)MEM – MIDAS – IP;
M3: MS(3)MEM – MIDAS – EMV; **M4**: MS(3)MEM – MIDAS – RV.
Light blue (common part), blue (specific part). Jan. 2, 2003 – Dec. 31, 2014.

(a) M1 vs M2

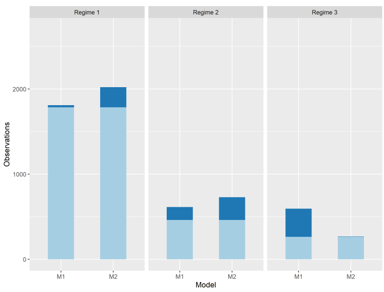

(b) M1 vs M3

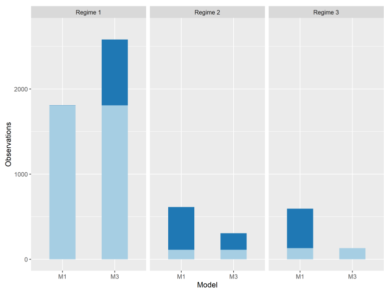

(c) M1 vs M4

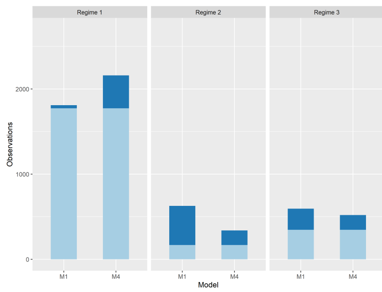

(d) M2 vs M3

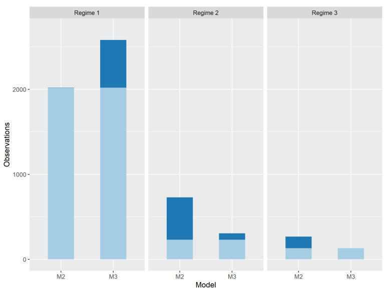

(e) M2 vs M4

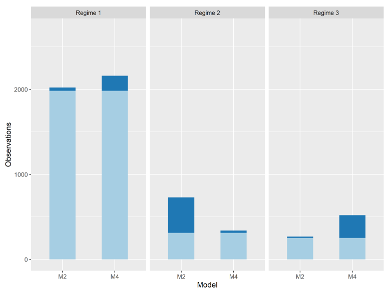

(f) M3 vs M4

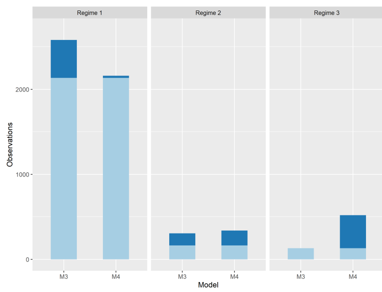

These results show that the choice of the low–frequency variable does induce different results in our MS(3) MEM–MIDAS models, and that the performance of the EMV mixed model is somewhat disappointing when it comes to discriminating across regimes. The RV mixed model has the highest value of the estimated log–likelihood function (cf. last line in Table 2).

This descriptive comparison is complemented by some histograms representing in Figure 4 the distribution of the volatility observations according to which regime they are classified by the four MS(3) models. In each panel, the red area corresponds to the low–volatility regime, the blue to the mid–volatility regime and the green to the high–volatility regime. This gives some interesting insights in how the values of volatility *per*

Figure 4: Volatility distribution across inferred regimes of four MS models. Low–volatility regime (red area), mid–volatility regime (blue area), high–volatility regime (green area). Sample: Jan. 2, 2003 – Dec. 31, 2014. Volatility Proxy: annualized Realized kernel Volatility.

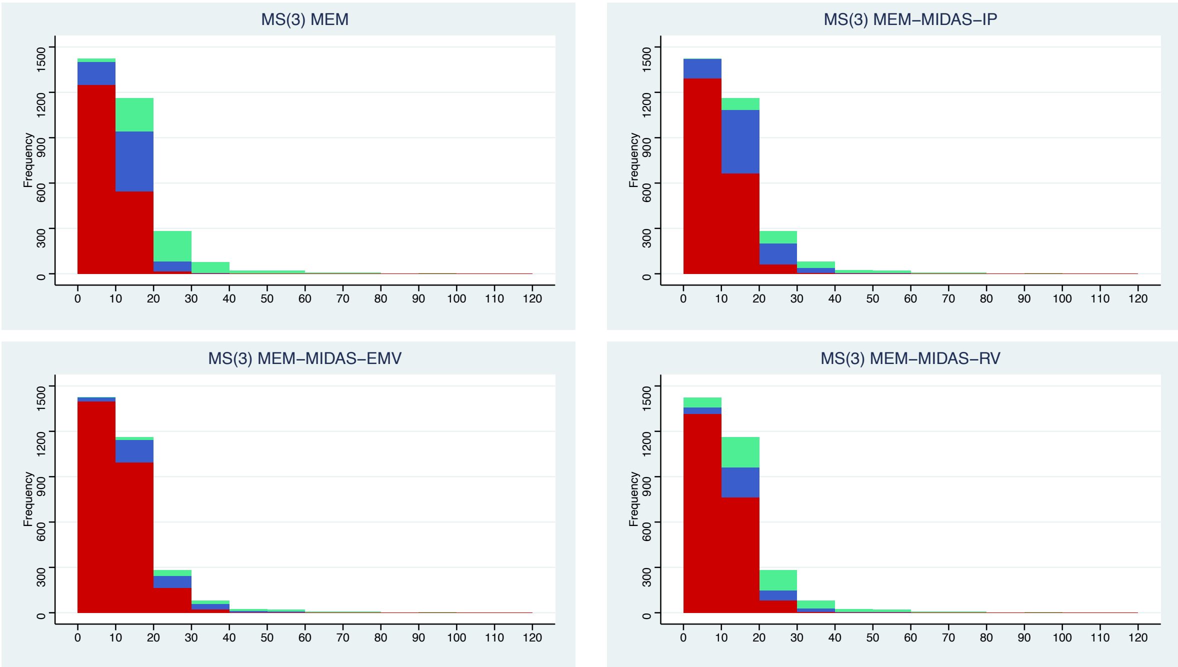

se are not sufficient to classify regimes: the allocation by each model depends on its capability to capture the evolution of the dynamics in reference to the prevailing average level of volatility, whereby some bursts in volatility, although smaller in size, are able to make the model switch to a higher state. In this respect, we recognize the EMV mixed model's tendency to characterize as low–volatility even values that are fairly sizeable, while over–characterizing, as already noted, the importance of Regime 1. The message here is therefore that MS models, possibly complemented by a low–frequency component, can help in devising the importance of considering volatility movements relative to the prevailing state in that moment.

A formal comparison among models can be carried out with an analysis of their in– and out–of–sample performance.

4.1 The in–sample performance

We report in–sample statistics in Table 5, where we calculate a few diagnostics, the value of the log–likelihood function, together with the Akaike and the Bayesian information criteria and a loss function used as reference (QLIKE) with further results discussed below. The MS(3) MEM-MIDAS-RV is the best model judging by the log–likelihood value and the AIC, as well as the QLIKE loss; in terms of BIC, the MEM-MIDAS-EMV shows the best performance.

The values of the QLIKE can be used to compare the in–sample performance of the estimated models through the Model Confidence Set (MCS) procedure of Hansen et al., 2011. To test the null hypothesis of equal predictive capacity, we employ the

Table 5: In–sample performance of the estimated models: Sample: Jan. 2, 2003 – Dec. 31, 2014.

	MEM	MEM MIDAS IP	MEM MIDAS EMV	MEM MIDAS RV	MS(3) MEM	MS(3) MEM MIDAS IP	MS(3) MEM MIDAS EMV	MS(3) MEM MIDAS RV
LOGLIK	-8611.61	-8578.42	-8537.78	-8539.33	-8509.89	-8489.82	-8483.89	**-8477.97**
AIC	5.714	5.693	5.666	5.667	5.657	5.645	5.641	**5.637**
BIC	5.724	5.707	**5.680**	5.681	5.699	5.691	5.687	5.683
QLIKE	7.450	7.291	7.102	7.109	7.044	6.964	6.928	**6.912**
Rank	8	7	5	6	4	3	2	1
p-value	0.014	0.014	0.014	0.014	0.044	0.405	0.666	1.000

By row, the best model is identified in boldface. LOGLIK: value of the maximized log-likelihood function; AIC: Akaike Information Criterion: BIC: Bayesian Information Criterion; QLIKE: Value of the Quasi-Likelihood function (multiplied by 100); Rank refers to the results of the Model Confidence Set approach and indicates the (inverse) order by which the models are removed (8 is the first model removed, 1 the best performing model) according to the QLIKE criterion; p-value is the corresponding MCS p-value.

semi–quadratic statistic:

$$T_{SQ} = \frac{\sum_{i \neq j} \bar{d}_{ij}^2}{\widehat{Var(\bar{d}_{ij})}}$$

where $\bar{d}_{ij}$ is the sample mean difference between the loss function series of models i and j, while $\widehat{Var(\bar{d}_{ij})}$ is the estimated variance of $\bar{d}_{ij}$ through a bootstrap procedure of 10000 resamples. When the null hypothesis is rejected, the worst model is eliminated and the test is repeated for the remaining models until the null hypothesis is not rejected, thus suggesting which models enter a set possessing equivalent predictive capability.

In this respect, the bottom part of Table 5 shows (row labeled *Rank*) the order by which the models are removed by the best set in terms of QLIKE loss function. Setting the significance level equal to 0.05, the best set is formed by the three MS(3) MEM-MIDAS, showing how the new models proposed provide the best fitting performance.

Comparatively speaking, the forecasting performance of the models can be evaluated also by calculating the Diebold and Mariano (DM – Diebold and Mariano, 1995) test statistics, still using QLIKE as the loss function of reference. In Table 6, we report the results for the in–sample period: as it often happens, the more parameterized models outperform the simpler ones: in particular, the MS(3)-MEM-MIDAS model with RV performs really well, beating all models, with an indistinguishable performance relative to the one with EMV.

Graphically, we can see that the models with Markovian dynamics and/or a mixed frequency component offer a more flexible pattern of the long–run component, that is, the average level around which conditional volatility fluctuates (Figure 5), relative to the base MEM.

The similarity of the long–run components can be better evaluated in terms of correlation coefficients. Table 7 shows all the correlations between the long–run components derived from each pair of models (excluding MEM, which is constant). We notice a strong correlation between the MEM-MIDAS-EMV and both MIDAS models that use RV as the

Table 6: p-values for the Diebold-Mariano test statistics under the null hypothesis of equal performance of the in–sample forecasts. Sample: Jan. 2, 2003 – Dec. 31, 2014.

QLIKE	MEM	MEM MIDAS IP	MEM MIDAS EMV	MEM MIDAS RV	MS(3) MEM	MS(3) MEM MIDAS IP	MS(3) MEM MIDAS EMV
MEM-MIDAS-IP	0.013						
MEM-MIDAS-EMV	0.017	0.031					
MEM-MIDAS-RV	0.026	0.054	0.594				
MS(3)-MEM	0.010	0.019	0.137	0.118			
MS(3)-MEM MIDAS-IP	0.007	0.009	0.010	0.006	0.030		
MS(3)-MEM-MIDAS-EMV	0.006	0.006	0.002	0.001	0.411	0.016	
MS(3)-MEM-MIDAS-RV	0.005	0.006	0.001	0.000	0.007	0.085	0.333

H_0 : QLIKE (row) = QLIKE (column); H_a : QLIKE (row) < QLIKE (column). In red p–values < 0.1 (model by row "wins" against model by column).

Figure 5: Estimated conditional volatility of four models. Realized Volatility (gray line), conditional volatility (blue line), long–run component (green line). Sample: Jan. 2, 2003 – Dec. 31, 2014. Volatility Proxy: annualized Realized kernel Volatility.

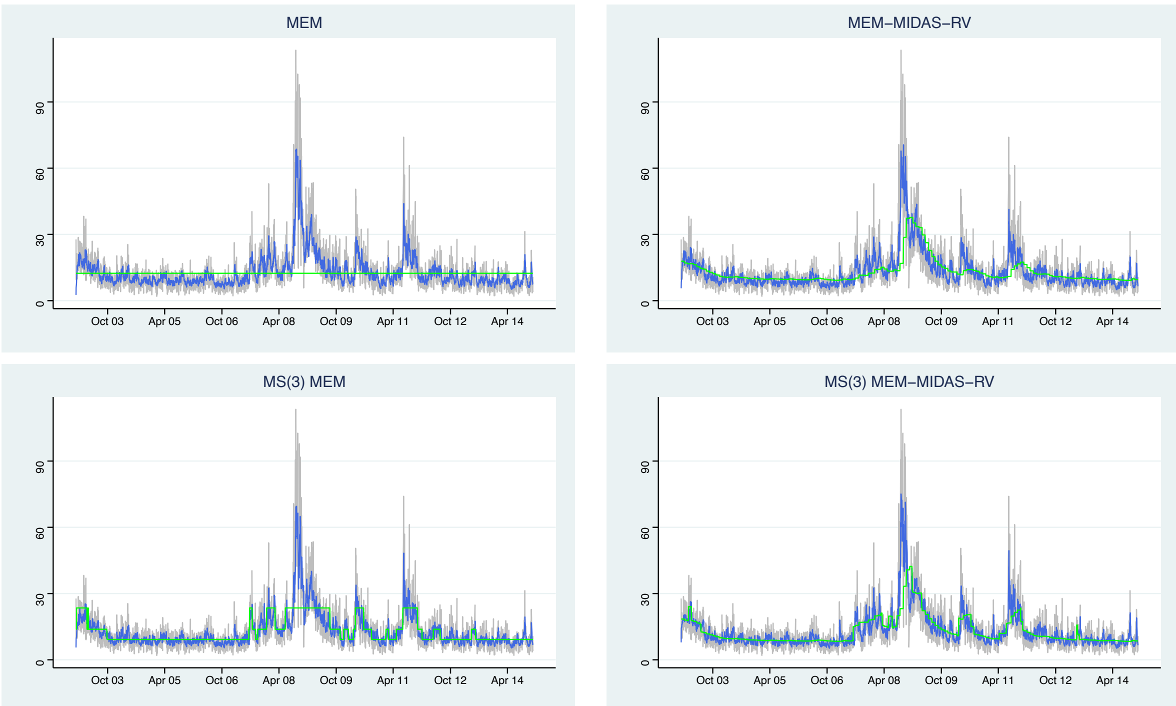

low–frequency variable. Apart from a lower correlation, between 0.55 and 0.63, between the MEM MIDAS-IP and each of the MS models, all pairs show a relatively high degree of linear relationship (16 out of 21 are greater than 0.73).

Table 7: Correlation coefficients among long–run components ($\tau_{i,t}$) derived from seven MIDAS models. Sample: Jan. 2, 2003 – Dec. 31, 2014.

	MEM MIDAS EMV	MEM MIDAS RV	MS(3) MEM	MS(3) MEM MIDAS IP	MS(3) MEM MIDAS EMV	MS(3) MEM MIDAS RV
MEM-MIDAS-IP	0.771	0.813	0.555	0.593	0.567	0.629
MEM-MIDAS-EMV		0.933	0.764	0.817	0.808	0.906
MEM-MIDAS-RV			0.682	0.732	0.739	0.880
MS(3) MEM				0.856	0.742	0.826
MS(3) MEM MIDAS IP					0.903	0.866
MS(3) MEM MIDAS EMV						0.821

4.2 The out–of–sample performance

The out–of–sample exercise is performed on a rolling window scheme for the period between January 2, 2015 and December 31, 2020. We start by generating the one step ahead forecasts for the year 2015 based on the first in–sample estimation period, then we shift forward the whole estimation period by one year and we re-estimate the model to produce the forecasts for the following year, and so on.

In this forecasting setup, looking at the Table 8, the MIDAS models making use of the IP overall fare poorly, showing the highest QLIKE loss function values. Repeating the MCS procedure for the out–of–sample results, we notice that the models entering the best set at 0.05 significance level are (in order of ranking) MS(3) MEM-MIDAS-RV, MS(3) MEM-MIDAS-EMV, MEM-MIDAS-RV, MS(3) MEM and MEM. However, one should notice the large difference in p–values between the MEM and the other models: if one were to use a significance level around 0.25, as suggested by some authors (for example, Hansen et al., 2011 themselves), in order to avoid the possibility of high first type error of sequential tests, the MEM would be excluded from the best set.

The results from the Diebold–Mariano test (see Table 9) support similar conclusions: the MIDAS models using IP fare poorly, overall, and the base MEM does not fare worse than some other richer models. The MS(3)-MEM-MIDAS with RV maintains the satisfactory performance (never dominated by others), showing that the addition of the Markov switching behavior generally adds relevant value in forecasting. By focusing on the last row of the table, the MS(3)-MEM-MIDAS with RV exhibits the best performance, beating most mixed–frequency models (with the exception of the one making use of the same variable RV) and having a similar performance as the MS(3) MEM and as the MS(3)-MEM-MIDAS with EMV.

5 Concluding remarks

The major contribution of this paper is to have introduced a new class of (asymmetric) Multiplicative Error Models in which we combine variables sampled at different frequency (in the MIDAS logic) with a Markovian dynamics (Markov switching): the behavior of the low–frequency component (monthly in the case of our application) is allowed to assume different values according to the latent regime prevailing at the daily level.

Table 8: Out of sample results: MCS p-values for the QLIKE. Forecasting Period: Jan. 2, 2015 – Dec. 31, 2020.

	MEM	MEM MIDAS IP	MEM MIDAS EMV	MEM MIDAS RV	MS(3) MEM	MS(3) MEM MIDAS IP	MS(3) MEM MIDAS EMV	MS(3) MEM MIDAS RV
QLIKE	6.955	7.297	7.025	6.834	6.845	7.040	6.825	**6.759**
Rank	5	8	6	3	4	7	2	1
p-value	0.139	0.000	0.036	0.557	0.557	0.010	0.557	1.000

QLIKE: value of the Quasi-Likelihood function (multiplied by 100). Rank indicates the (inverse) order in which the models are removed in the MCS approach (7 is the first model removed, 1 the best performing model); p-value is the corresponding MCS p-value. Boldface for the best model by row.

Table 9: Diebold-Mariano test: p-value under the null hypothesis of equal performance of the out of sample forecasts. Forecasting Period: Jan. 2, 2015 – Dec. 31, 2020.

QLIKE	MEM	MEM MIDAS IP	MEM MIDAS EMV	MEM MIDAS RV	MS(3) MEM	MS(3) MEM MIDAS IP	MS(3) MEM MIDAS EMV
MEM-MIDAS-IP	1.000						
MEM-MIDAS-EMV	0.764	0.014					
MEM-MIDAS-RV	0.018	0.000	0.003				
MS(3)-MEM	0.130	0.001	0.073	0.548			
MS(3)-MEM-MIDAS-IP	0.793	0.005	0.547	0.980	0.957		
MS(3)-MEM-MIDAS-EMV	0.092	0.000	0.014	0.452	0.411	0.016	
MS(3)-MEM-MIDAS-RV	0.023	0.000	0.004	0.165	0.113	0.000	0.142

p-value of the Diebold and Mariano test. H_0 : QLIKE (row) = QLIKE (column); H_a : QLIKE (row) < QLIKE (column). In red p–values < 0.1 (model by row "wins" against model by column); in blue p–values > 0.90 (model by column "wins" against model by row).

In this specification of the Markov switching MEM-MIDAS, the Markov chain regulating the dynamics of the realized volatility is the same for both the low– and the high–frequency components. An interesting extension to be investigated is to allow the Markovian dynamics to be different across components (taking on the logic adopted by Sola et al., 2002 and Gallo and Otranto, 2008 in different contexts).

The results provide an alternative to working with either type of MEM (MIDAS or MS) taken in isolation, leading to a more flexible representation of the underlying dynamics of the slow–moving component, a common characteristic exhibited by financial volatility over a long period. It also allows for an economic interpretation of what moves the average level of volatility: given that the most satisfactory forecasting performance appears to involve the MS(3)-MEM-MIDAS with RV, which uses monthly realized volatility as the driving variable for the low–frequency component, in this case an aggregation of what is available at a higher frequency provides some useful insights as of the overall dynamics.

The volatility considered here is measured on the S&P 500 index, which involves one of the most important markets and has a widespread basis of stock in its composition: however, the analysis conducted on different US indices or different markets would not necessarily reach the same conclusions, and this suggests further empirical investigations about the relative merits of these models.

References

Amendola, A., Candila, V., Cipollini, F., & Gallo, G. M. (2021). Doubly multiplicative error models with long–and short–run components. *Technical Report*.

Amendola, A., Candila, V., & Gallo, G. M. (2019). On the asymmetric impact of macro–variables on volatility. *Economic Modelling*, *76*, 135–152.

Andersen, T. G., & Bollerslev, T. (1998). Answering the skeptics: Yes, standard volatility models do provide accurate forecasts. *International Economic Review*, *39*, 885–905.

Andersen, T. G., Bollerslev, T., Diebold, F. X., & Labys, P. (2003). Modeling and forecasting realized volatility. *Econometrica*, *71*, 579–625.

Baker, S. R., Bloom, N., Davis, S. J., & Kost, K. J. (2019). Policy news and stock market volatility. *NBER Working Paper No. 25720*.

Balzanella, A., Bini, M., Cavicchia, C., & Verde, R. (Eds.). (2022). *Sis 2022: Book of the short papers*. Pearson.

Barndorff-Nielsen, O. E., Hansen, P. R., Lunde, A., & Shephard, N. (2008). Designing realised kernels to measure the ex-post variation of equity prices in the presence of noise. *Econometrica*, *76*, 1481–1536.

Bollerslev, T., Patton, A. J., & Quaedvlieg, R. (2016). Exploiting the errors: A simple approach for improved volatility forecasting. *Journal of Econometrics*, *192*, 1–18. http://www.sciencedirect.com/science/article/pii/S0304407615002584

Bollerslev, T., & Wooldridge, J. M. (1992). Quasi-maximum likelihood estimation and inference in dynamic models with time-varying covariances. *Econometric Reviews*, *11*, 143–172.

Brownlees, C. T., Cipollini, F., & Gallo, G. M. (2012). Multiplicative error models. In L. Bauwens, C. Hafner, & S. Laurent (Eds.), *Volatility models and their applications* (pp. 223–247). Wiley.

Cipollini, F., & Gallo, G. M. (2022). Multiplicative error models: 20 years on. *Econometrics and Statistics*. https://www.sciencedirect.com/science/article/pii/S2452306222000740

Cipollini, F., Gallo, G. M., & Otranto, E. (2021). Realized volatility forecasting: Robustness to measurement errors. *International Journal of Forecasting*, *37*(1), 44–57. http://www.sciencedirect.com/science/article/pii/S0169207020300467

Conrad, C., & Kleen, O. (2020). Two are better than one: Volatility forecasting using multiplicative component garch-midas models. *Journal of Applied Econometrics*, *35*(1), 19–45.

Diebold, F. X., & Mariano, R. S. (1995). Comparing predictive accuracy. *Journal of Business & Economic Statistics*, *13*(3), 253–263.

Engle, R. F., & Lee, G. J. (1999). A permanent and transitory component model of stock return volatility. In R. F. Engle & H. White (Eds.), *Cointegration, causality, and forecasting: A festschrift in honor of clive w. j. granger* (pp. 475–497). Oxford University Press.

Engle, R. F. (2002). New frontiers for ARCH models. *Journal of Applied Econometrics*, *17*, 425–446.

Engle, R. F., & Gallo, G. M. (2006). A multiple indicators model for volatility using intra-daily data. *Journal of Econometrics*, *131*, 3–27.

Engle, R. F., Ghysels, E., & Sohn, B. (2013). Stock market volatility and macroeconomic fundamentals. *Review of Economics and Statistics*, *95*(3), 776–797.

Engle, R. F., & Russell, J. R. (1998). Autoregressive conditional duration: A new model for irregularly spaced transaction data. *Econometrica*, *66*, 1127–62.

Gallo, G. M., & Otranto, E. (2008). Volatility spillovers, interdependence and comovements: A Markov switching approach. *Computational Statistics & Data Analysis*, *52*(6), 3011–3026.

Gallo, G. M., & Otranto, E. (2015). Forecasting realized volatility with changing average levels. *International Journal of Forecasting*, *31*, 620–634.

Gallo, G. M., & Otranto, E. (2018). Combining sharp and smooth transitions in volatility dynamics: a fuzzy regime approach. *Journal of the Royal Statistical Society Series C*, *67*(3), 549–573.

Hamilton, J. D. (1994). *Time series analysis*. Princeton University Press.

Hansen, P. R., Lunde, A., & Nason, J. M. (2011). The model confidence set. *Econometrica*, *79*(2), 453–497.

Hubert, L., & Arabie, P. (1985). Comparing partitions. *Journal of Classification*, *2*, 193–218.

Kim, C. (1994). Dynamic linear models with Markov switching. *Journal of Econometrics*, *60*, 1–22.

Kolmogorov, A. (1933). Sulla determinazione empirica di una legge di distribuzione. *Giornale dell'Istituto Italiano degli Attuari*, *4*, 83–91.

Manganelli, S. (2005). Duration, volume and volatility impact of trades. *Journal of Financial Markets*, *8*, 377–399.

Officer, R. R. (1973). The variability of the market factor of the New York Stock Exchange. *The Journal of Business*, *46*(3), 434–453.

Pan, Z., Wang, Y., Wu, C., & Yin, L. (2017). Oil price volatility and macroeconomic fundamentals: A regime switching GARCH-MIDAS model. *Journal of Empirical Finance*, *43*, 130–142.

Rand, W. M. (1971). Objective criteria for the evaluation of clustering methods. *Journal of the American Statistical Association*, *66*, 846–850.

Schwert, G. W. (1989). Why does stock market volatility change over time? *Journal of Finance*, *44*(5), 1115–1153.

Sola, M., Spagnolo, F., & Spagnolo, N. (2002). A test for volatility spillovers. *Economics Letters*, *76*(1), 77–84.

Wang, F., & Ghysels, E. (2015). Econometric analysis of volatility component models. *Econometric Theory*, *31*(2), 362–393.

Ultimi Contributi di Ricerca CRENoS

I Paper sono disponibili in: http://www.crenos.unica.it

22/04 *Claudio Detotto, Riccardo Marselli, Bryan C. McCannon, Marco Vannini,* "Experts and Arbitration Outcomes: Insights from Public Procurement Contract Disputes"

22/03 *Gerardo Marletto, Cécile Sillig,* "Global influence and national diversity in socio-technical transitions: a sectoral taxonomy"

22/02 *Federico Aresu, Emanuela Marrocu, Raffaele Paci,* "Public capital and institutions' quality in the Italian regions"

22/01 *Gabriele Cardullo, Maurizio Conti, Andrea Ricci, Sergio Scicchitano, Giovanni Sulis,* "On the Emergence of Cooperative Industrial and Labor Relations"

21/11 *Gianfranco Atzeni, Luca G. Deidda, Marco Delogu, Dimitri Paolini,* "Effects of migration with endogenous labor supply and heterogeneous skills"

21/10 *Alberto Tidu, Stefano Usai, Frederick Guy,* "Agglomeration in manufacturing and services: an experimental application of a distance-based measure to Sardinia"

21/09 *Andrea Caria, Fabio Cerina, Marco Nieddu,* "Political Selection and Monetary Incentives in Local Parliamentary Systems"

21/08 *Giorgio Garau, Alessio Tola, Maria Veronica Camerada, Salvatore Lampreu, Silvia Carrus,* "Economic and social polarization dynamics in the EU"

21/07 *Emanuela Marrocu, Raffaele Paci, Stefano Usai,* "Direct and indirect effects of universities on European regional productivity"

21/06 *Pasqualina Arca, Gianfranco Atzeni, Luca Deidda,* "The Signalling Role of Trade Credit on Loan Contracts: Evidence from a Counterfactual Analysis"

21/05 *Grazia Sveva Ascione, Laura Ciucci, Claudio Detotto, Valerio Sterzi,* Do universities look like patent trolls? An Empirical Study of University Patent Infringement Litigation in the United States

21/04 *Michele Battisti, Massimo Del Gatto, Antonio Francesco Gravina, Christopher F. Parmeter,* "Robots versus labor skills: a complementarity / substitutability analysis"

21/03 *William Addessi, Marco Delogu,* "Infrastructure Accumulation in Developing Countries: the Role of the Informal Sector"

21/02 *Luca De Benedictis, Vania Licio, Anna Maria Pinna,* "From the historical Roman road network to modern infrastructure in Italy"

21/01 *Silvia Balia, Rinaldo Brau, Marco G. Nieddu,* "Depowering Risk: Vehicle Power Restriction and Teen Driver Accidents in Italy"

20/08 *Giampiero M. Gallo, Demetrio Lacava, Edoardo Otranto,* "On Classifying the Effects of Policy Announcements on Volatility"

20/07 *Luc Bauwens, Edoardo Otranto,* "Modelling Realized Covariance Matrices: a Class of Hadamard Exponential Models"

20/06 *Demetrio Lacava, Giampiero M. Gallo, Edoardo Otranto,* "Measuring the Effects of Unconventional Policies on Stock Market Volatility"

20/05 *Gianfranco Atzeni, Luca G. Deidda, Marco Delogu, Dimitri Paolini,* "Drop-out decisions in a cohort of Italian university students"

20/04 *Emanuela Marrocu, Raffele Paci, David Rigby, Stefano Usai,* "Smart Specialization Strategy: any relatedness between theory and practice?

20/03 *Giorgio Garau, Stefano Deriu,* "Total Factor Productivity and Relative Prices: the case of Italy"

20/02 *Fabio Cerina, Alessio Moro, Michelle Rendall,* "A Note on Employment and Wage Polarization in the U.S."

20/01 *Elias Carroni, Dimitri Paolini,* "Business models for streaming platforms: content acquisition, advertising and users" www.crenos.unica.it

ISBN 9788868514372